

## TEM Characterization of a $\text{Mg}_2\text{Si}_{0.5}\text{Sn}_{0.5}$ Solid Solution for High-Performance Thermoelectrics

Minghui Song,<sup>1</sup> Ji-Wei Liu,<sup>1</sup> Masaki Takeguchi,<sup>1</sup> Naohito Tsujii,<sup>2</sup> and Yukihiro Isoda<sup>3</sup>

<sup>1</sup> Transmission Electron Microscopy Station, National Institute for Materials Science (NIMS), 1-2-1 Sengen, Tsukuba, Ibaraki 3050047 Japan.

<sup>2</sup> Quantum Beam Unit, NIMS, 1-2-1 Sengen, Tsukuba, Ibaraki 3050047 Japan.

<sup>3</sup> Battery Materials Unit, NIMS, 1-2-1 Sengen, Tsukuba, Ibaraki 3050047 Japan.

Intermetallic compounds of  $\text{Mg}_2\text{X}$  ( $\text{X} = \text{Si}, \text{Sn}$  or  $\text{Ge}$ ) are promising thermoelectric materials in the intermediate temperature range (400–800 K) because of their good electrical properties, low lattice thermal conductivity, and potentially high thermoelectric performance [1]. Studies have demonstrated that in the  $\text{Mg}_2\text{Si}_{1-x}\text{Sn}_x$  system,  $x \approx 0.5$  is one of the best choices for achieving a high thermoelectric performance of the material, because the large atomic mass difference between Si and Sn dramatically reduces the thermal conductivity of the solid solutions, which leads to a high value of figure of merit,  $ZT$ , of about 1.1 near 800 K [2]. The thermoelectric properties of these materials strongly depend on the local microstructure. Therefore, precisely understanding of the microstructure and composition of the material is essentially important for the development of high performance materials. In the present work, a  $\text{Mg}_2\text{Si}_{0.5}\text{Sn}_{0.5}$  solid solution was characterized with TEM and other related methods, in scales from nanometer to sub-millimeter.

A  $\text{Mg}_2\text{Si}_{0.5}\text{Sn}_{0.5}$  solid solution was prepared by mixing  $\text{Mg}_2\text{Si}$  and  $\text{Mg}_2\text{Sn}$  powders and hot-pressing the mixture [3]. The starting materials were powder of Mg (purity 99.9%), Si (99.9999%), and Sn (99.999%).  $\text{Mg}_2\text{Si}$  and  $\text{Mg}_2\text{Sn}$  alloys were synthesized by the liquid-solid reaction and the melting reaction methods, respectively. The obtained  $\text{Mg}_2\text{Si}$  and  $\text{Mg}_2\text{Sn}$  ingots were ground, mixed, and hot-pressed under Ar atmosphere at 80 MPa and 1068 K for 50 h. Structural and compositional characterization was carried out with XRD, SEM, electron probe microanalysis (EPMA), and TEM. The TEM observation and analysis were performed on a TEM, JEM-2100F (JEOL Co. Ltd.) operated at 200 kV. TEM specimens were prepared in two ways. One was the FIB method using a 30 keV  $\text{Ga}^+$  ion beam (JEOL, JIB-4000). Another way was to crush bulk materials to powders in sub-micrometer size and load the powder on polymer microgrids.

XRD confirmed the successful synthesis of the  $\text{Mg}_2\text{Si}_{0.5}\text{Sn}_{0.5}$  solid solution which was in an antiferroite structure. The samples exhibited a much lower thermal conductivity ( $1.92 \text{ W m}^{-1} \text{ K}^{-1}$  at 300 K) than the parent  $\text{Mg}_2\text{Si}$  ( $8.75 \text{ W m}^{-1} \text{ K}^{-1}$ ) and  $\text{Mg}_2\text{Sn}$  compounds ( $6.28 \text{ W m}^{-1} \text{ K}^{-1}$ ). The low thermal conductivity of  $\text{Mg}_2\text{Si}_{0.5}\text{Sn}_{0.5}$  resulted in a relatively high  $ZT = 0.0132$  at 300 K. SEM revealed that the grains were mainly 10–20  $\mu\text{m}$  in size and had clean grain boundaries without obvious inclusions and precipitates. EPMA analysis at points and for elemental mappings revealed that the relative differences in composition between grains could reach several percents, and that there were differences in composition at grain boundaries and inside the grains. Figure 1 shows the EPMA elemental mappings. TEM and STEM observations revealed that there were typical two kinds of grains, structurally homogeneous and heterogeneous ones. Almost no large inclusions were observed in the former grains, while inclusions of Si and Sn in size from tens to hundreds of nanometers were observed in the later grains. Furthermore, in both kinds of grains, high density MgO nanoparticles 10–20 nm in size were observed which dispersed evenly in the grains. Figure 2 shows the TEM images, and the selected area diffraction patterns (SADP)

of a specimen prepared with FIB from a homogeneous grain. When the specimen was observed in a direction out of a low index zone axis, diffraction rings were observed which were from tiny MgO particles. The bright dots observed in the dark field image were MgO nano particles which distributed evenly in the specimen. The Oxygen and/or MgO may be originated from the starting materials or the atmosphere during the synthesis process. Dispersed MgO nano particles could decrease the thermal conductivity since they scatter phonons, therefore, they might be beneficial to the thermoelectric performance of the material. The reasons for the MgO nano particles to distribute dispersely in grains may be that the alloying during the hot-press was processed partially in solid state. The existence of the unreacted Si and Sn inclusions and the heterogeneous in elemental distribution convinced that there is still a space to improve the thermoelectric performance of the materials by optimizing the synthesis procedure, alloy composition, and doping level, etc. [4]

#### References:

- [1] W. Liu, *et al*, *Chem. Mater.* **23** (2011), p. 5256.
- [2] V. K. Zaitsev, *et al*, *Phys. Rev. B* **74** (2006), p. 045207.
- [3] J. W. Liu, *et al*, *J. Electronic Mater.* **44** (2015), p. 407.
- [4] Thanks to Mitsuaki Nishio in NIMS for his help and discussion on the EPMA analysis.

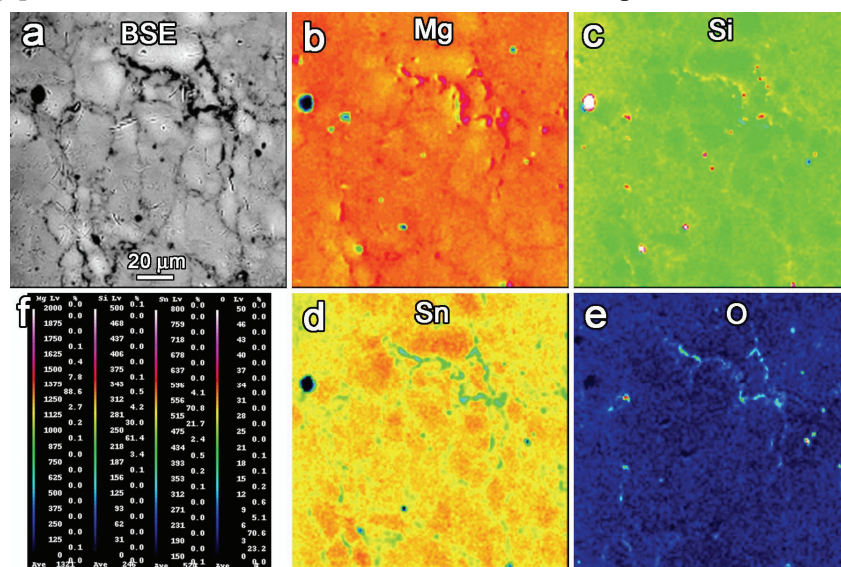


**Figure 1.** EPMA (electron probe microanalysis) elemental mappings of a  $\text{Mg}_2\text{Si}_{0.5}\text{Sn}_{0.5}$  specimen. (a) Backscattered electron image; (b-e) Mappings of Mg, Si, Sn, and O, respectively; (f) Intensity scales of the mappings.

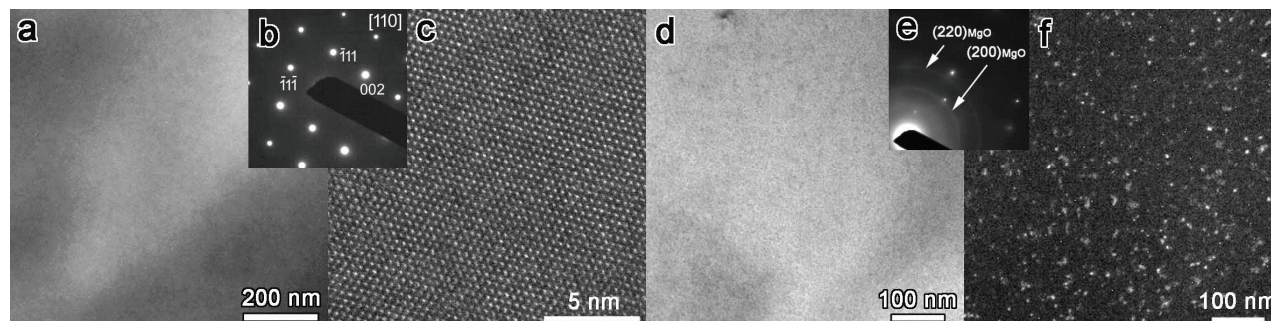


**Figure 2.** TEM images of a  $\text{Mg}_2\text{Si}_{0.5}\text{Sn}_{0.5}$  specimen. (a-c) The BF (bright field), the SADP (selected area diffraction pattern), and high resolution transmission electron microscopy images observed in direction of [110]; (d-f) The BF, SADP, and dark field images observed in a direction out of a low index zone axis.